Theoretical calculation of frequencies and thresholds of microwave-induced auditory signals

James C. Lin

Department of Electrical and Computer Engineering, Wayne State University, Detroit, Michigan 48202

Previously developed thermoelastic models of microwave-induced auditory sensations are applied to calculate the frequency and amplitude of the acoustic signals that are generated in human beings and laboratory animals. Graphs of computed displacement and pressure as a function of time are presented for several species.

1. INTRODUCTION

Auditory sensations are produced in human beings and in animals that are irradiated with rectangular pulses of microwave radiation of high peak density [*Frey*, 1961; *Frey and Messenger*, 1973; *Guy et al.*, 1973, 1975; *Taylor and Ashleman*, 1974; *Rissman and Cain*, 1975; *Chou et al.*, 1975, 1976]. Several physical mechanisms of interaction have been considered in attempts to account for the conversion of microwaves to acoustic energy [*Sommer and Von Gierke*, 1964; *Foster and Finch*, 1974; *Sharp et al.*, 1974; *Guy et al.*, 1975]. Recently, a comparison of the pressure amplitude as produced in a semi-infinite layer of homogeneous brain material that is irradiated by a microwave pulse indicated that the peak pressure due to thermal expansion is much greater than either radiation pressure or electrostriction [*Lin*, 1975, 1976]. A theoretical model based on thermal expansion has therefore been developed for spherical heads that are irradiated by pulsed microwave energy [*Lin*, 1977a,b]. Some experimental data obtained by others were compared and were found to agree favorably with preliminary calculations, thus indicating the usefulness of the model.

In this paper the theoretical formulation is applied to the heads of cats and of guinea pigs irradiated by 2450-MHz microwaves and to heads of infants and adult human beings exposed to 918-MHz radiation in order to obtain displacement data and pressure waveforms. The data are of value in estimating the characteristics of acoustic signals that are generated in standard laboratory animals and human subjects. They may also serve as a guide to the design of laboratory experiments that are aimed at resolving the exact mechanism of interaction in terms of the signal levels and frequency responses of test instruments. Furthermore, the results will be useful to individuals concerned with establishing a realistic safety standard for microwave radiation.

2. THEORY

The explicit expressions for the acoustic waves that are generated in a spherical model of the head as irradiated by rectangular pulses (t_0 = pulse width) of microwave energy have previously been presented [*Lin*, 1977a,b]. Briefly, it was shown that the pattern of absorbed energy inside a spherical head may be approximated by the spherically symmetric function $\sin(N\pi r/a)/(N\pi r/a)$ for many combinations of sizes and frequencies, where r is the radial variable, a is the radius of the sphere, and N is the number of standing-wave-like oscillations in the absorption pattern.

Taking advantage of the symmetry of the absorption pattern and assuming that thermal conduction does not take place within the short periods of time under consideration, the inhomogeneous thermoelastic equation of motion was solved for the acoustic wave parameters under both stress-free and constrained-surface conditions. In particular, it was found that under the stress-free assumption the fundamental frequency of sound generated in the head without shear stress is given by

$$f_{1f} = c_1/2a \tag{1}$$

where c_1 is the velocity of bulk acoustic-wave propagation in brain material. The displacement is given by

$$u_f = u_0\, Qt + \sum_{m=1}^{\infty} A_m j_1(k_m r)(\sin\omega_m t/\omega_m), \quad 0 \leqslant t \leqslant t_0 \tag{2}$$

$$u_f = u_0\, Qt_0 + \sum_{m=1}^{\infty} A_m j_1(k_m r)[(\sin\omega_m t)/\omega_m - \sin\omega_m (t-t_0)/\omega_m], \quad t \geqslant t_0 \tag{3}$$

and the radial stress (pressure) is

$$\sigma_f = 4\mu\, u_0\, St + \sum_{m=1}^{\infty} A_m k_m M_m (\sin\omega_m t/\omega_m), \quad 0 \leqslant t \leqslant t_0 \tag{4}$$

$$\sigma_f = 4\mu u_0 S t_0 + \sum_{m=1}^{\infty} A_m k_m M_m [(\sin\omega_m t)/\omega_m - \sin\omega_m (t-t_0)/\omega_m], \quad t \geqslant t_0 \tag{5}$$

where

$$u_0 = (I_0/\rho c_h)[\beta/(\lambda+2\mu)] \tag{6}$$

$$Q = (a/N\pi)j_1(N\pi r/a) \pm [4\mu/(3\lambda+2\mu)]\,[r/(N\pi)^2] \tag{7}$$

$$S = \pm (1/N\pi)^2 - j_1(N\pi r/a)\,/\,(N\pi r/a) \tag{8}$$

$$M_m = [(\lambda+2\mu)j_0(k_m r) - 4\mu j_1(k_m r)/(k_m r)] \tag{9}$$

and

$$A_m = \mp 2u_0 a/(N\pi)^2 \{[4\mu/(3\lambda+2\mu)]\,[j_2(k_m a)/(k_m a) - k_m a j_0(k_m a)/[(k_m a)^2 - (N\pi)^2]]\}/ \{[j_1(k_m a)]^2 - j_0(k_m a)j_2(k_m a)\} \tag{10}$$

for $k_m a = m\pi$. In cases where $m\pi = N\pi$, equation (10) reduces to

$$A_m = -u_0 a/(N\pi)\,[1 + 24u/(3\lambda+2\mu)(1/N\pi)^2] \tag{11}$$

The upper sign in equations (7) to (10) and in subsequent expressions denotes $N = 1, 3, 5, \ldots$ and the lower sign denotes $N = 2, 4, 6, \ldots$

The fundamental frequency of sound generated in a spherical head with constrained boundary but without shear stress was shown to be given by

$$f_{1c} = 4.49\, c_1/(2\pi a) \tag{12}$$

which is higher than that predicted by equation (1) under stress-free conditions. The radial displacement for constrained surfaces is given by

$$u = u_0 D t + \sum_{m=1}^{\infty} A_m j_1(k_m r)(\sin\omega_m t/\omega_m), \quad 0 < t < t_0 \tag{13}$$

$$u = u_0 D t_0 + \sum_{m=1}^{\infty} A_m j_1(k_m r)[\sin\omega_m t/\omega_m - \sin\omega_m (t-t_0)/\omega_m], \quad t > t_0 \tag{14}$$

and the pressure is

$$\sigma = u_0 G t + \sum_{m=1}^{\infty} A_m k_m H_m (\sin\omega_m t/\omega_m), \quad 0 < t < t_0 \tag{15}$$

$$\sigma = u_0 G t_0 + \sum_{m=1}^{\infty} A_m k_m H_m [\sin\omega_m t/\omega_m - \sin\omega_m (t-t_0)/\omega_m], \quad t > t_0 \tag{16}$$

where

$$D = (1/N\pi)[a j_1(N\pi r/a) \mp (r/N\pi)], \tag{17}$$

$$G = -(4\mu a/N\pi r)j_1(N\pi r/a) \mp (1/N\pi)^2(3\lambda+2\mu) \tag{18}$$

$$H_m = (\lambda+2\mu)j_0(k_m r) - (4\mu/k_m r)j_1(k_m r) \tag{19}$$

$$A_m = \pm 2u_0 a(1/N\pi)^2 \{(1/k_m a)j_2(k_m a) \pm k_m a j_0(k_m a)/ [(k_m a)^2 - (N\pi)^2]\}/\{[j_1(k_m a)]^2 - j_0(k_m a) j_2(k_m a)\} \tag{20}$$

In the following section, equations (1) through (20) are applied to obtain detailed numerical results for the frequency, displacement and sound pressure generated in the heads of guinea pigs and cats exposed to 2450-MHz radiation and in the heads of infants and adult human beings exposed to 918-MHz radiation. The necessary thermoelastic parameters of brain material are given in Table 1. Note that μ is very small compared to λ.

3. NUMERICAL RESULTS

3.1. *Frequency.*

It is observed readily from equations (1) and (12) that the frequency of sound is a function only of the head and of brain tissue acoustic properties. It does not depend at all on characteristics of microwave absorption. Clearly, the acoustic pitch perceived by a given subject will be the same regardless of the frequency of the impinging microwave radiation.

A comparison of fundamental frequency as a function of radius is shown in Figure 1. It is seen that the frequency varies inversely with radius; the smaller the radius, the higher the frequency. Note that the fundamental frequency predicted by the constrained-surface formulation is about 70% higher than that computed from the stress-free expression. Since the head is not perfectly spherical and the surface may best be described as semi-rigid, it is possible that the actual curve of the fundamental frequency of sound resides somewhere between the two curves that are shown in Figure 1.

TABLE 1. Thermoelastic properties of brain matter [*Lin*, 1977a].

Specific Heat, c_h	0.88 cal/g-°C (0.21 J/g-°C)
Density, ρ	1.05 g/cm^3
Coefficient of Thermal Expansion, α	4.1 × 10^{-5}/°C
Lame's Constant, λ	2.24 × 10^{10} dyn/cm^2
Lame's Constant, μ	10.52 × 10^3 dyn/cm^2
Bulk Velocity of Propagation, c_1	1.46 × 10^5 cm/s

If we choose the median of these two curves, it can be seen that, for a guinea pig (a = 2 cm), the predicted fundamental frequency is 45 kHz, which is close to that measured by *Chou et al.* [1975]. For a typical cat (a = 3 cm) the measured cochlear microphonic frequency is 38 kHz. Figure 1 shows a computed frequency of 30 kHz. The computed frequency for an infant (a = 5 cm) and an adult human being (a = 7 cm) are 18 and 13 kHz, respectively. Although experimental data that are directly applicable to this case are not available, related results have indicated that a necessary condition for auditory perception by adults seems to be the ability to hear sounds above 5 to 8 kHz [*Frey*, 1961; *Rissmann and Cain*, 1975].

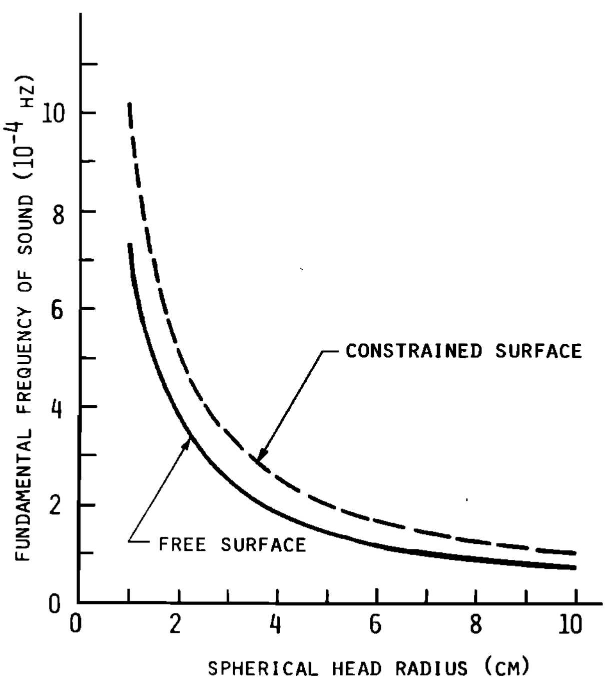

Fig. 1. Predicted fundamental frequency of vibration of a spherical head in a pulse-moderated microwave field.

3.2. *Peak pressure and displacement.*

Extensive numerical computations have shown that, although the resultant waveforms are qualitatively similar, both pressures and displacements that are computed on the basis of the constrained-surface formulation are consistently higher than those calculated using the stress-free expressions. Moreover, better agreement between theory and experiment exists for the constrained-boundary formulation. The following presentation is therefore specifically related to the constrained-boundary expressions given by equations (13) to (20).

Figures 2 and 3 show the peak pressure and displacement at r = 0, 1 and 2 cm for a sphere of 2-cm radius that stimulates the head of a guinea pig under 2450-MHz radiation. In this case the approximate microwave absorption pattern is obtained by setting N = 3. These waveforms are evaluated for t_0 = 10 μsec. It is seen that the pressure is the highest at the center of the head and has a maximum value of 4.08 dyne/cm^2 for a peak absorption rate of 1 W/g (which corresponds to a power density 445 mW/cm^2 of incident energy [*Johnson and Guy*, 1972]) at the end of the pulse and then oscillates around a constant average value in the absence of elastic damping. As expected, the displacement is zero both at the center and at the surface of the sphere for the constrained-boundary condition. The peak displacement at r = 1.0 cm is about 2.16 X 10^{-13} meters. Note that a high-frequency component is superimposed on top of the fundamental frequency, which correlates perfectly with that shown in Figure 1.

The peak pressure and displacement at r = 0, 1.5 and 3.0 cm for a 3-cm sphere, which simulates the head of a cat exposed to 2450-MHz radiation, are illustrated in Figures 4 and 5. In this case the approximate microwave absorption pattern is obtained by setting N = 6. Again, the pressure is the highest at the center, and has a value of 3.69 dyne/cm^2 for a peak absorption rate of 1 W/g or 589 mW/cm^2 of incident energy. Quantitative comparisons with two series of experimental threshold determinations [*Guy et al.* 1975; *Rissmann and Cain*, 1975] indicate that the computed threshold is extremely close to the measured ones [*Lin*, 1977b]. The displacement in the model of the cat's head is about 1.51 X 10^{-13} meters. The fundamental frequency of oscillation ob-

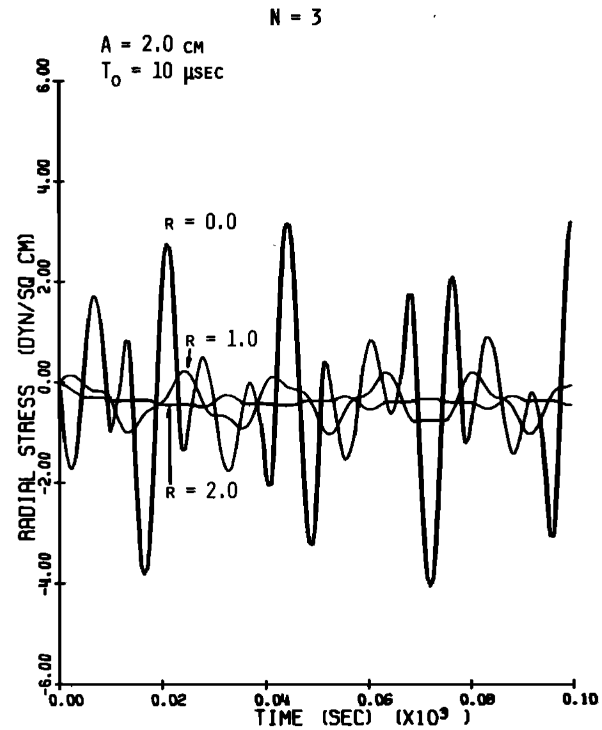

Fig. 2. Sound pressure generated in a sphere of 2-cm radius that stimulates a guinea pig's head exposed to 2450-MHz radiation. The peak absorption rate is 1000 mW/cm^3. For other parameters see text.

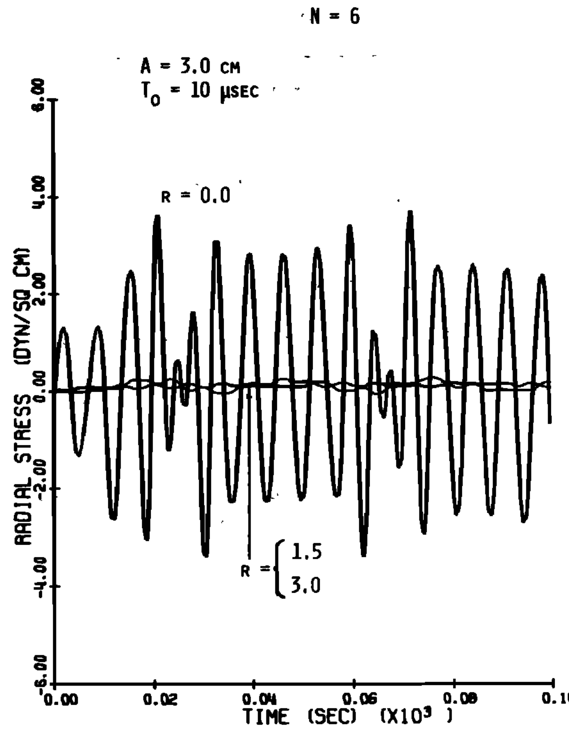

Fig. 4. Sound pressure generated in a sphere of 3-cm radius that simulates a cat's head exposed to 2450-MHz radiation.

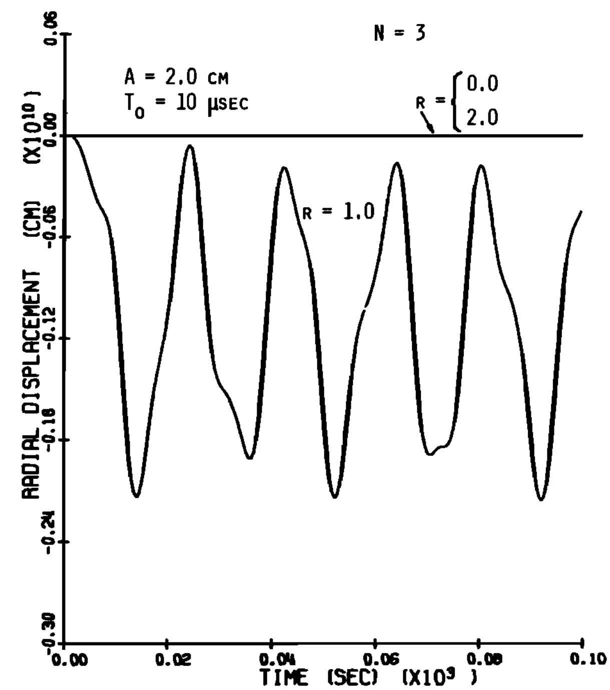

Fig. 3. Displacement produced in a spherical head of 2-cm radius (compare with Fig. 2).

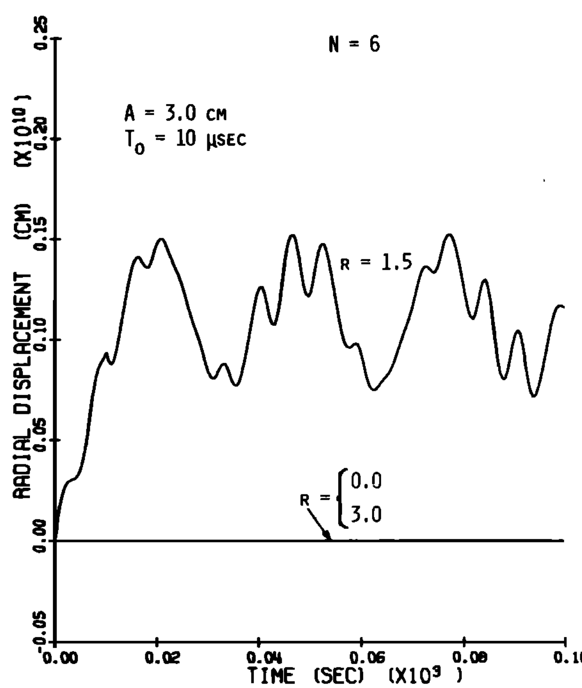

Fig. 5. Displacement produced in a spherical head of 3-cm radius.

tained from Figure 5 agrees well with that given in Figure 1.

For a 5-cm sphere that simulates the head of an infant exposed to 918-MHz radiation, the peak pressure at the center is 9.61 dyne/cm^2 as seen from Figures 6 and 7. This curve was obtained by letting $N = 3$ in the approximated microwave-absorption pattern. The displacement in this case is approximately 9.34×10^{-13} m for a peak absorption of 1 W/g and an incident power density of 1282 mW/cm^2. As before, the pulse width is assumed to be 10 μsec. Again, good agreement is found between the fundamental frequency of mechanical oscillation and that predicted in Figure 1 for a 5-cm sphere.

Figures 8 and 9 present the pressure and displacement in a 7-cm sphere that simulates the head of an adult irradiated by 918-MHz microwaves. Again, the pulse width is 10 μsec and the peak absorption is 1 W/g, which corresponds to 2183 mW/cm^2 of incident plane wave power. The calculated peak pressure is 6.82 dyne/cm^2 and the displacement is about 3.97×10^{-13} meters. A careful examination reveals that the pressure values obtained are in qualitative agreement with results obtained experimentally at 1245-MHz [*Frey and Messenger*, 1973; *Lin*, 1976c]. It should be noted that specific measurements of the human response to 918-MHz radiation have not been reported to date.

Table 2 is a summary of peak pressures and displacements in four animals as irradiated by 10-μsec pulses at the same level of absorbed energy. The incident power

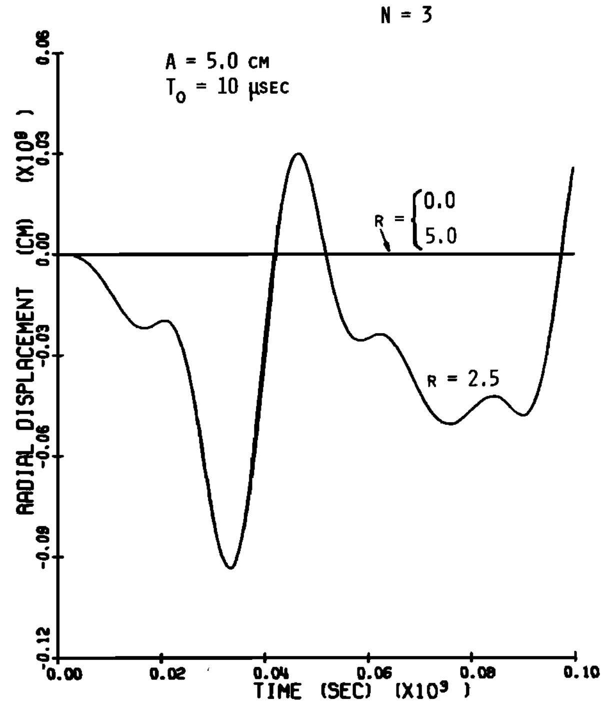

Fig. 7. Displacement produced in a spherical head of 5-cm radius.

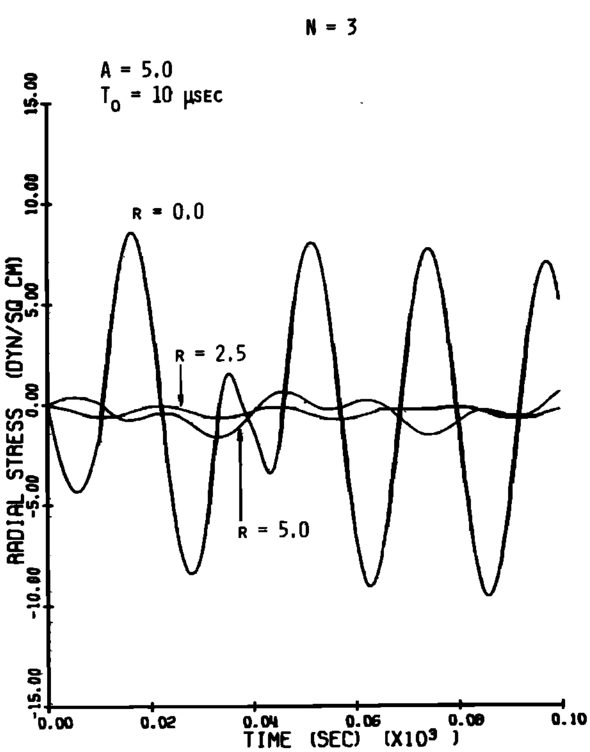

Fig. 6. Sound pressure generated in a sphere of 5-cm radius that simulates a human infant's head exposed to 918-MHz radiation.

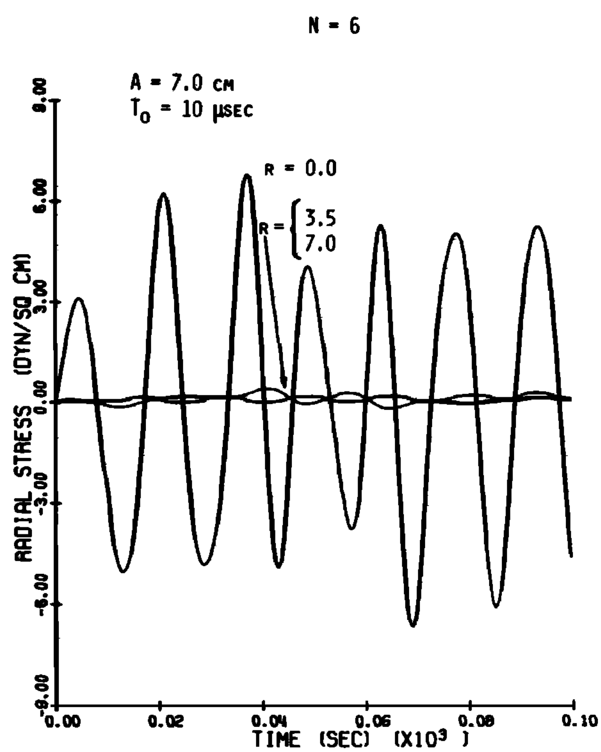

Fig. 8. Sound pressure generated in a sphere of 7-cm radius that simulates a human adult's head exposed to 918-MHz radiation.

TABLE 2. Peak pressure and displacement in spherical head models irradiated with 10 μsec rectangular microwave pulses at a peak absorption rate of 1 W/g.

Sphere Radius (cm)	Microwave Frequency (MHz)	Species	Pressure (dyne/cm^2)	Displacement (10^{-11} cm)	Incident Power (mW/cm^2)
2	2450	guinea pig	4.08	2.16	445
3	2450	cat	3.69	1.51	589
5	918	human infant	9.61	9.34	1282
7	918	human adult	6.82	3.97	2183

density and the frequency differ according to the species involved. Although the pulse width and peak absorption rate are the same in each case, the pressure and displacement differ somewhat. These data will enable experimenters to estimate the peak pressure that is expected for a given power density of incident energy.

4. CONCLUSIONS

The thermoelastic model for microwave-induced auditory sensations was used to calculate acoustic-wave characteristics in human beings and common laboratory animals that are exposed to pulsed microwaves. Quantitative estimates of the frequency and amplitude of induced pressure and displacement have been obtained for guinea pigs, cats, infants and adult human beings under irradiation by 2450- and 918-MHz microwaves.

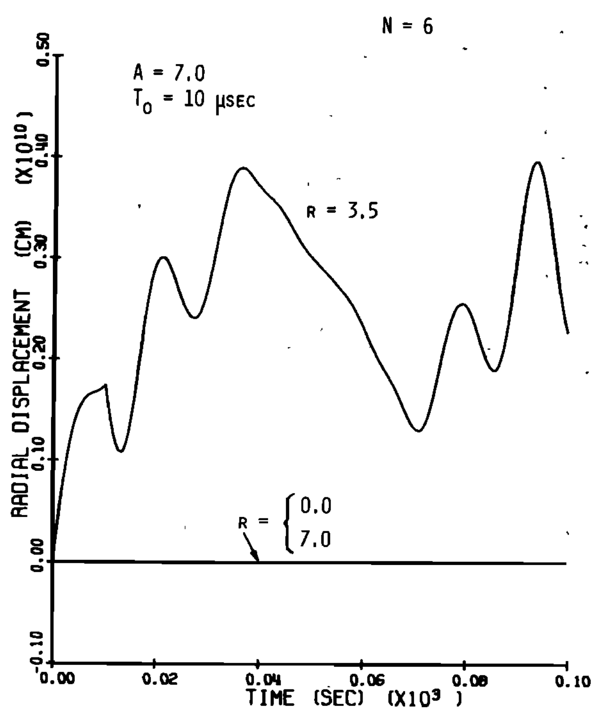

Fig. 9. Displacement produced in a spherical head of 7-cm radius.

The tabulated data and graphical presentations will be useful to investigators who are interested in pursuing threshold studies for exposure to microwave radiation. They may also serve as a guide to the design of laboratory experiments that are aimed at resolving the exact mechanism of interaction in terms of the signal levels and frequency responses of test instruments.

ACKNOWLEDGMENT. This work was supported in part by National Science Foundation Grant ENG 75-15227.

REFERENCES

Chou, C. K., R. Galambos, A. W. Guy, and R. H. Lovely (1975), Cochlear microphonics generated by microwave pulses, *J. Microwave Power, 10,* 361-367.
Chou, C. K., A. W. Guy, and R. Galambos (1976), Microwave-induced cochlear microphonics in cats, *J. Microwave Power, 11,* 171-173.
Foster, K. R., and E. D. Finch (1974), Microwave hearing: evidence for thermo-acoustical auditory stimulation by pulsed microwaves, *Science, 185,* 256-258.
Frey, A. H. (1961), Auditory system response to radio-frequency energy, *Aerosp. Med., 32,* 1140-1142.
Frey, A. H., and R. Messenger, Jr. (1973), Human perception of illumination with pulsed ultra-high frequency electromagnetic energy, *Science, 181,* 356-358.
Guy, A. W., E. M. Taylor, B. Ashleman, and J. C. Lin (1973), Microwave interaction with the auditory systems of humans and cats, *IEEE/MTT Int. Symp. Digest,* 321-323.
Guy, A. W., C. K. Chou, J. C. Lin, and D. Christensen (1975), Microwave induced acoustic effects in mammalian auditory systems and physical materials, *Ann. N.Y. Acad. Sci., 247,* 194-215.
Johnson, C. C., and A. W. Guy (1972), Nonionizing electromagnetic wave effects in biological materials and systems, *Proc. IEEE, 60,* 692-718.
Lin, J. C. (1975), Biomedical effects of microwave radiation - a review, *Proc. Nat. Electron. Conf., 30,* 224-232.
Lin, J. C. (1976), Microwave auditory effect - a comparison of some possible transduction mechanisms, *J. Microwave Power, 11,* 77-81.
Lin, J. C. (1977a), On microwave-induced hearing sensation, *IEEE Trans. Microwave Theory Tech., 25,* 605-613.
Lin, J. C. (1977b), Further studies on the microwave auditory effect, *IEEE Trans. Microwave Theory Tech., 25,* 936-941.
Rissmann, W. J., and C. A. Cain (1975), Microwave hearing in mammals, *Proc. Nat. Electron. Conf., 30,* 239-244.
Sharp, J. C., H. M. Grove, and O. P. Gandhi (1974), Generation of acoustic signals by pulsed microwave energy, *IEEE Trans. Microwave Theory Tech., 22,* 583-584.
Sommer, H. C., and H. E. Von Gierke (1964), Hearing sensations in electric field, *Aerosp. Med., 35,* 834-839.
Taylor, E. M., and B. T. Ashleman (1974), Analysis of the central nervous involvement in the microwave auditory effect, *Brain Res., 74,* 201-208.